

## Corrosion protection of Stainless Steel Used in Orthopedic Implants by Chemical and Physical Treatment

*E. A. Ayob<sup>1-2</sup>, D. M. El-zeer<sup>3-4</sup>, and O. S. Shehata<sup>5</sup>*

<sup>1</sup>Taif University, Faculty of Science and Education in Al-khurma (girls branch), Chemistry Dep., Al-khurma, KSA

<sup>2</sup>Nuclear and Radiological Regulatory Authority, Nasr City, Cairo, Egypt

<sup>3</sup>Taif University, Faculty of Science and Education in Al-khurma (girls branch), Physics Dep., Al-khurma, KSA

<sup>4</sup>Center of plasma technology, Al-Azhar Univesity, Nasr City, Cairo, Egypt

<sup>5</sup>Physical Chemistry Department, National Research Centre, Dokki, Giza, Egypt

---

Copyright © 2015 ISSR Journals. This is an open access article distributed under the *Creative Commons Attribution License*, which permits unrestricted use, distribution, and reproduction in any medium, provided the original work is properly cited.

**ABSTRACT:** Austenitic Stainless Steel is one of the most widely used biomaterials for implants process, In the present study chemical and physical treatment have been used on two types of austenitic Stainless, 316L and 310S to compare their corrosion performance on both samples before and after both treatments. Corrosion rate for two samples was decrease with both treatments; polarization is confirming the open circuit potential and weight loss results. Metallography was studied by electron microscopy and X-ray photoelectron spectroscopy (XPS) method to evaluate the effectiveness of the proposed method and to determine the chromium concentration in the surface layer after treatment.

**KEYWORDS:** Stainless steel, Biomaterials, Chemical Treatment, Physical Treatment, XPS.

### 1 INTRODUCTION

One of the most important process in developing medical science is Orthopedic Implants. The first requirement for any material to be placed in the human body is that it should be biocompatible and not cause any adverse reaction in the body, this materials names is biomedical materials. Stainless steel 316L are one of the most widely used biomaterials for implants process, because of its capability to resist corrosion, mechanical properties and cheaper price according to another materials. Corrosion test is important consideration for a material used as biomedical materials because metal ion release takes place mainly due to corrosion of surgical implants. The first requirement for any material to be placed in the human body is that it should be biocompatible and not cause any adverse reaction in the body. The material must withstand the body environment and not degrade to a point that it cannot function in the body as intended [1]. Metallic materials are widely used as biomedical materials and are indispensable in the medical field. In particular, toughness, elasticity, rigidity, and electrical conductivity are essential properties for metallic materials used in medical devices [2, 3]. The performance of a biomaterial is determined by its chemical, physical and biological properties [4]. In the complex environment of the human body, biomedical materials are subject to electrochemical corrosion mechanisms, with bodily fluids acting as an electrolyte [5-8].

Corrosion is the first consideration for a material of any type that is to be used in the body because metal ion release takes place mainly due to corrosion of surgical implants [9] and it can adversely affect the biocompatibility and mechanical integrity [1] and the high concentration of Cl<sup>-</sup> and the temperature range of 36.7–37.2°C, the human body fluid is considered a severely corrosive environment and localized corrosions such as pitting and crevice corrosion [10]. Stainless steel are used

as temporary implants to help bone healing, as well as fixed implants such as for artificial joints. In terms of corrosion resistance in the human body, stainless steels are inferior compared to cobalt chromium alloys and titanium alloys [11-14]. However, large amounts of stainless steel are used for implant devices because they are less expensive than cobalt-chromium alloys, pure titanium, and titanium alloys [15].

Presence of Cr results in the formation of a thin, chemically stable, and passive oxide film on the surface of the stainless steels [16, 17]. The oxide film forms and heals itself in the presence of oxygen. The physical-chemical properties of this passive film control the material's corrosion behavior, its interaction with the body, and thus the degree of the material's biocompatibility [18]. There have been numerous in-vivo and in-vitro studies focused on corrosion in metal implants. However, many of the in-vitro studies employed simulated body fluids such as Ringer's or Hanks' solutions [19]. It has been reported that corrosion resistance of stainless steel is closely related to chromium concentration in the film formed by surface treatment methods [20-22]. The aim of this research is to compare the electrochemical corrosion behaviours of 316L and 310S stainless steel alloys using Tafel Extrapolation, weight loss test before and after chemical and physical (plasma) surface treatment. The metallography by electron microscopy were used to evaluate the effectiveness of the proposed method. X-ray photoelectron spectroscopy (XPS) method was used to determine the chromium concentration in the surface layer after surface treatment.

## 2 MATERIALS AND METHODS

### 2.1 MATERIALS PREPARATION

Materials used in this research were two different types of Austenitic Alloys AISI types 316L, 310S which was cut into small sheets of dimensions 15x 20 x2 mm, their chemical composition of samples are presented in Table 1. Prior to each experiment the electrode surface was mechanically abraded with 400 up to 2000, grit emery papers, rinsed with distilled water, degreased in acetone, absolute ethanol and dried in air. The biological fluid test is Hank's solution at pH 7.4, the chemical compositions of it is shown in Table 2 [19]. The cell used contained typically three electrode for electrochemical measurement. The counter electrode was made of platinum, saturated calomel electrode (SCE) as a reference electrode and the samples as the working electrode, the exposed area into test solution was 1cm<sup>2</sup>.

### 2.2 SURFACE TREATMENT

Surface treatments were employed for all test samples of stainless steel: Mechanical Polish, Chemical Polish, Chemical Polish & Passivation and Physical Treatment by plasma. Chemical Passivation was carried out in a glass cell under certain conditions as presented in Table 3. The samples were washed, cleaned and dried with hot air after surface treatment. Physical Treatment (plasma) employed in the discharge cell which consists of two movable parallel electrodes enclosed in a cylindrical Pyrex glass tube of 7 cm diameter and 20 cm length. Each electrode consists of a disk made of steel of 4 cm in diameter. The stainless steel samples were pasted to the cathode by silver paste. The temperature of the sample is controlled by using an electric heater that is placed under the cathode. The glass tube is evacuated by using a vacuum system to a base pressure about  $2 \times 10^{-3}$  Torr. A mixture of N<sub>2</sub>-H<sub>2</sub> gases are entered the tube through needle valves (type Leybold AG 283 40) to control the pressure, and the percentage of the gas mixture inside the reactor. The temperature of the cathode is measured by a copper-constantan thermocouple imbedded in the cathode. The two electrodes are connected to the dc power supply of variable output voltage. Two types of stainless steel samples have been treated by plasma. The stainless steel samples are treated under the same conditions that are placed in the Table 3.

*Table 1. Chemical composition of different types of austenitic steel in the present study.*

Type of steel	C	Cr	Ni	Mo	Mn	P	Si	S	Fe
316 L	0.021	17.7	10.5	2.76	1.56	0.017	0.71	0.002	66.73
310 S	0.08	25	20	0.3	0.1	0.0425	0.85	0.02	53.6

**Table 2. Chemical compositions of Hank's solution.**

Compound	Composition (g/l)
NaCl	8.00
KCl	0.40
CaCl <sub>2</sub>	0.14
NaHCO <sub>3</sub>	0.35
Na <sub>2</sub> HPO <sub>4</sub> ·2H <sub>2</sub> O	0.06
KH <sub>2</sub> PO <sub>4</sub>	0.60
MgSO <sub>4</sub> ·7H <sub>2</sub> O	0.06
MgCl <sub>2</sub> ·6H <sub>2</sub> O	0.10
Glucose	1.00

**Table 3. Surface treatment conditions for all stainless steel types**

Sample name	Treatment types	Treatment Condition				
MP	Mechanical polish	used SiC papers of number 400,600,1000, 1200 and 2000				
CP	Chemical polish	12.5 ml HNO <sub>3</sub> + 4 ml HF + 33.5 ml H <sub>2</sub> O at 30°C for 20 min.				
CP+P	Chemical polish + Passivation	12.5 ml HNO <sub>3</sub> + 4 ml HF + 33.5 ml H <sub>2</sub> O at 30°C for 20 min. Then passive in 30% HNO <sub>3</sub> at 70 °C for 20 min				
PT	Plasma treatment	N <sub>2</sub> :H <sub>2</sub> %	Discharge current (mA)	Temp. (°C)	time (sec)	Total pressure of the gases mixture (Torr)
		80:20	30	500	30	4

### 2.3 ELECTROCHEMICAL MEASUREMENT

All the measurements was performed at the Open Circuit Potential and Potentiodynamic Polarization, the data were obtained in the range of potentials from 1.5 to -1.6 V vs. SCE with the scan rate of 1 mV/s. at 37°C the device used is the workstation Auto lap 302N potentiostat/galvanostat instrument, Corrosion current density ( $i_{corr}$ ) which is equivalent to the corrosion rate of the specimen was estimated using Tafel extrapolation.

### 2.4 WEIGHT LOSS MEASUREMENT

The decrease in metal weight during the reference time period called weight loss methods was recorded by immersed the samples in Hank's solution during 200 days at temperature 37°C ±2 by water bath after clean with water, alcohol and degreased in acetone and dried in 100°C and then weighted before and after exposure

### 2.5 MICROSTRUCTURE ANALYSIS

Composition of sample surface after treatment studied by the scanning electron microscope (SEM) Micrographs was collected using A JEOL JSM-5300 instrument attached by OXFORD and X-Ray photoelectron spectroscopy (XPS).

## 3 RESULTS AND DISCUSSION

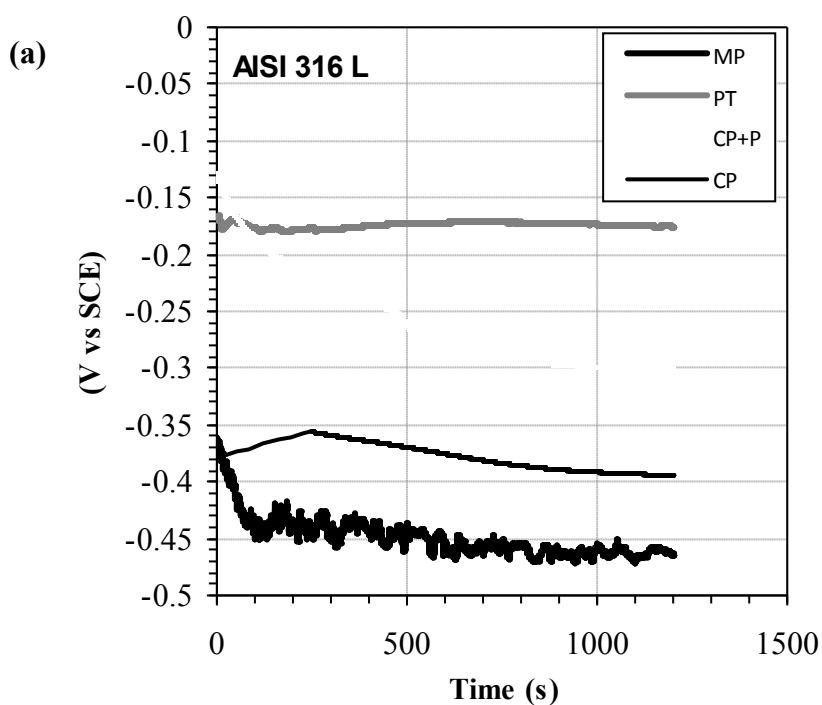
### 3.1 ELECTROCHEMICAL MEASUREMENT

#### 3.1.1 OPEN CIRCUIT POTENTIAL MEASUREMENTS

When a metal is immersed in a given solution, electrochemical reactions of the metal-solution interface occur at the surface of the metal, causing corrosion of the metal. These reactions create an corrosion potential or the open circuit potential (measured in volts), at the metal-solution interface [23]. The simple way determine the chemical interaction of metallic materials/bone prosthesis with the body fluid environment is essential in order to understand their stability in the human body and to study the film formation and passivity of implants/alloys in a Hank's solution.

Measurement open-circuit electrode potentials OCP as function of time is important for estimating the effect of depolarizers of corrosion reactions and useful to detect the initiation or an accelerated attack. An increase of open-circuit potentials OCP means depolarization of cathode and increase corrosion, a drop in potential is evidence for decreased corrosion. The rapid changes in the corrosion potential indicate a depolarization or enhancement of the anodic reaction, or to the formation of a semi-protective film [24].

An open circuit potential OCP as a function of time over 1200 S for two different types of stainless steel after Mechanical Polishing (MP), Chemical Polishing (CP), Chemical Polishing+Passive (CP+P) and Plasma Treated (PT) in the Hank's solution is provided in Fig.1. The evolution with time for the OCP ( $E_{oc}$ ) for AISI 316L SS samples are shown in Fig.1 a. It seems that, the potential is nearly constant after Plasma Treatment (PT) which means almost quasi-stationary state. The initial  $E_{oc}$  value shifts continuously towards the negative direction of potential with a faster rate and then slowly until it reaches steady state after Mechanical Polishing (MP) also after Chemical Polishing and Passive (CP+P) due to formation of a semi-protective film but the initial  $E_{oc}$  value shifts continuously towards the positive direction of potential with a faster rate and then to negative direction with slow rate until it reaches an almost quasi-stationary state after Chemical Polishing (CP). Samples can be arranged according to the shift of  $E_{oc}$  potential towards the positive direction with time as follow MP, CP, CP+P, PT



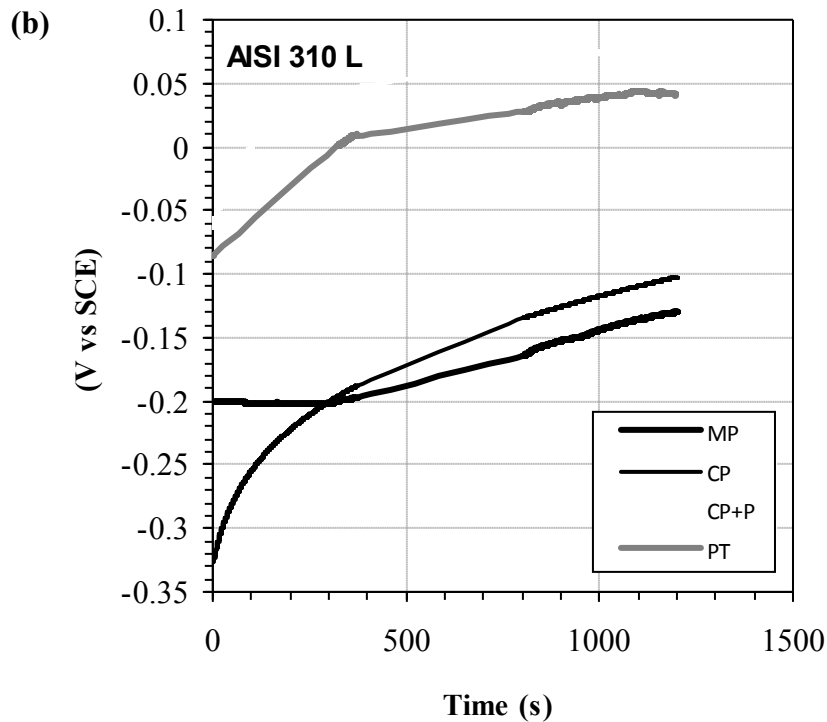


**Fig. 1.** Evolution of the open circuit potential ( $E_{oc}$ ) for both Stainless Steel samples at different treatment conditions in Hank's solution (a) AISI 316 L stainless steel and (b) AISI 310 S stainless steel

As shown in Table 4a. While Samples can be arranged according to the shift of  $E_{oc}$  potential towards the positive direction with time as follow MP, CP, PT and CP+P respectively as shown in Table 4b. This indicates a propensity for the sample to passivity due to its interaction with test solution and deposition of protective corrosion products according to types of surface treatment. The evolution with time for the OCP ( $E_{oc}$ ) can be shown for AISI 310S SS in Fig. 1 b, As can be seen, the initial  $E_{oc}$  value shifts continuously towards the positive direction of potential with a faster rate and then slowly until it reaches an almost quasi-stationary state after all surface treatments. Values of the  $E_{oc}$  implies that CP+P sample possesses thicker native oxide film relative to PT sample which is relative to CP sample which is relative to that for MP sample respectively.

In general it can be noticed that the  $E_{oc}$  more positive potential for AISI 310S SS samples than for AISI 316L SS samples. This implies that AISI 316L SS samples possess thicker native oxide film relative to AISI 310S SS, while for AISI 316L SS samples, the ion has initially to penetrate an oxide film corresponding to high anodic polarization with respect to AISI 310S. Shifting the potential to more positive or negative values is not a main factor affected on the corrosion rate. This is because thickness alone is not assumed to provide a criterion of protection, as the kinetics of attack is related to a variety of other factors such as surface film composition, microstructure, continuity and adhesion to the substrate [25, 26]. The nature of the formed film being protective will be further clarified based on the data of potentiodynamic polarization techniques.

### 3.1.2 POTENTIODYNAMIC POLARIZATION MEASUREMENTS

It is a technique where the potential of the electrode is varied at a selected rate by application of a current through the electrolyte, the polarization curves usually show linear behavior of  $E$  vs.  $\log(i)$ . This is called Tafel behavior. The anodic and cathodic polarization linear curves are extrapolated to  $E_{corr}$  to get  $i_{corr}$ . The electrochemical parameters obtained from the polarization curves for both AISI stainless steel samples after all surface treatment types have been reported in Table 4. These include the corrosion potential ( $E_{corr}$ ), the corrosion current density ( $i_{corr}$ ), anodic and cathodic Tafel slopes ( $\beta_a$ ,  $\beta_c$ ), breakdown potential and current ( $E_{bd}$ ,  $i_{bd}$ ) and the corrosion rate (CR). In some cases, the corrosion potentials are somewhat more negative than those obtained from the OCP measurements. This is because the polarization scans were started at a more cathodic potential relative to the OCP, so that the passive film at the surface was at least partially removed due to the highly reducing initial potential [27,28]. The potentiodynamic polarization scans (Tafel curves) for both stainless steel types after surface treatments; Mechanical Polishing (MP), Chemical Polishing (CP), Chemical Polishing+Passivity (CP+P) and

Plasma Treated (PT) in Hank's solution behave a very similar manner. The curves can be divided in several potential domains. In the cathodic domain where at this potential, the current can determined by the reduction of water and partially of dissolved oxygen. Another potential domains is transition domains which the cathodic current change to anodic current at the corrosion potential, in this intersection can be obtain current density of corrosion [29] The another domains corresponds to the passive plateau, before passivity was broken due to pitting corrosion is anodic domains. The smooth transition from domains potential to another occurs in all stainless steel types after all surface treatments were shown in Fig. 2. It can be seen from Fig. 2a that corrosion potential for 316L is arranged according to nobler (more positive) first, PT next, CP+P then, CP and finally, MP indicating that former is more corrosion resistant than later respectively. In Fig. 2b the corrosion potential for 310S is nobler (more positive) first, CP+P next, PT then, CP and finally, MP indicating that former is more corrosion resistant than later respectively.

We notice sharp increase after  $E_{corr}$  with a very small break in the current and well-defined current plateau after  $E_{corr}$  suggesting the existence of a partially protective film on the alloy surface [30, 31]. This domain corresponds to an apparent passivation zone, where the duration of its current plateau is very dependent on the solution composition and its aggressive nature. Over the potential region of the passive current zone a steady state is established between the rates of metal dissolution and passive film formation. Generally, the breakdown potential ( $E_{bd}$ ) of a given metal or alloy in corrosive environments is considered as an indication of the capability of its anodic passive film to resist localized corrosion damage [30, 32] and it is the major factor for selecting biomedical materials applications at the critical potential value  $E_{bd}$  breakdown of the passive film through its defective sites would expose the underneath substrate to the corrosive environment. Therefore, a more positive  $E_{bd}$  for surface treatment alloy in a test solution implies that its formed anodic film is more stable in terms of its localized corrosion performance and minimum corrosion rate accrued at sample. The maximum values of  $E_{bd}$  is observed for 316L stainless steel after treated by PT, and followed treated by CP+P, and followed treated by CP. The minimum  $E_{bd}$  is observed for 316L SS after treated by MP only. The maximum corrosion a rate was observed for the 316L SS after treated by MP, then treated by CP, and then treated by CP+P, and the last is PT. The maximum values of  $E_{bd}$  is observed for 310S stainless steel after treated by CP+P, and followed treated by PT, and followed treated by CP. The minimum  $E_{bd}$  is observed for 310S SS after treated by MP. The maximum corrosion rates was observed for the 310S SS after treated by MP, then treated by CP, then treated by PT, and the last is CP+P.

It can be possible obtain the anodic and cathodic Tafel slops for each stainless steel types at every surface treatment from polarization curves , it was possible analytically determinate the value of corrosion rate by using Stern-Geary[33].

$$I_{corr} = \frac{\beta_a \times \beta_c}{2.303 \times [\beta_a + \beta_c]} \times \frac{1}{R_p} \tag{1}$$

Where  $R_p$  is the polarization resistance,  $\beta_a$  and  $\beta_c$  are the anodic and cathodic Tafel slopes. From corrosion potential values, it was possible demonstrate that treatments types affected the electrochemical behaviour, in this sense the Fig. 3 shows the relation of corrosion rate with different types of treatment for both stainless steel. From values of polarization resistance it could be possible to determinate a porosity factor according with other authors [34, 35]. The total film porosity factor calculated from Eq. (2), it correspond to the ratio between the polarization resistance of abrasive sample (MP) and the other polishing treatments CP, CP+P and PT.

$$P = R_{pr-u} / R_{pr-u} \tag{2}$$

Where  $P$  is the total porosity,  $R_{pr-u}$  is the polarization resistance of mechanical polishing and  $R_{pr-u}$  is the measured polarization resistance of other polishing treatments. Fig. 4 represents the porosity factor values obtained replacing the electrochemical values of Eq. (3) for each treatment types.

$$Ef\% = \frac{I_{corr\ free} - I_{corr}}{I_{corr\ free}} \times 100 \tag{3}$$

Where  $E_f$  is the total protective efficiency,  $I_{corr}$  is the corrosion intensity of the mechanical polishing, and  $I_{corr\ free}$  is the corrosion intensity of the other polishing treatments.

**3.2 WEIGHT LOSS MEASUREMENT**

Fig. 5. represent the corrosion rate-time curves for both stainless steel types treated by MP, CP and CP+P. It can be seen from the figures, the corrosion rate decrease in both SS samples prepare under all treatment types by increasing the immersion time. The corrosion rate is function of weight loss according to Eq. (4). The decreasing of corrosion rate is confirming the open circuit potential and polarization results, that the samples reach steady state potentials. It can be seen

from the Fig. 5, the CP+P treated types have lower CR with respect CP and MP is almost higher corrosion rate in both SS types. The verity of corrosion rate according to stainless steel types and surface treatment are mainly caused by selective dissolution of iron in both SS types and surface treatment and therefore surface treatment of samples because passive layer

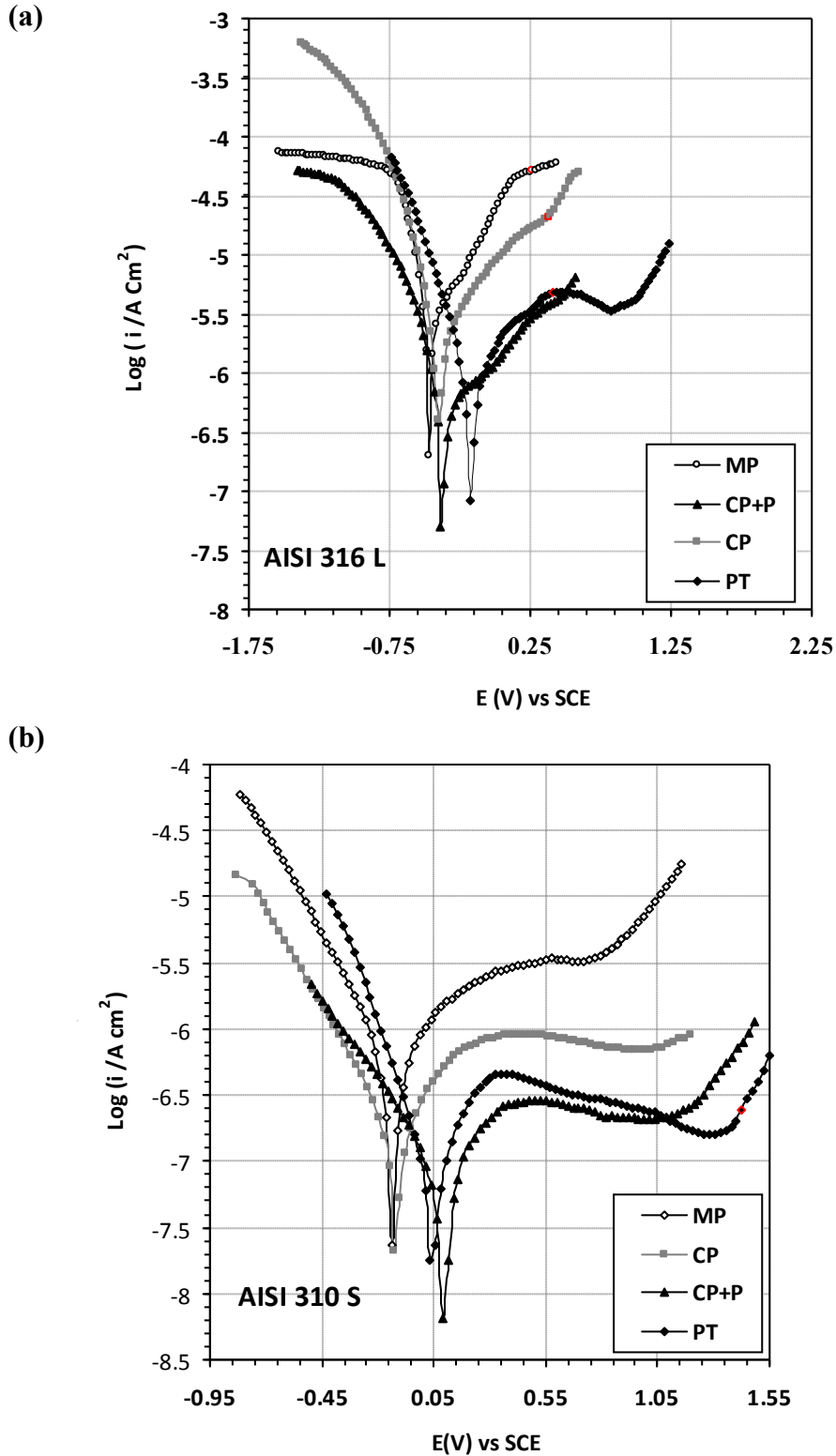


Fig. 2. Potentiodynamic polarization curves for both types of Stainless Steel at different treatment conditions in Hank's solution  
(a) AISI 316 L SS and (b) AISI 310 SS.

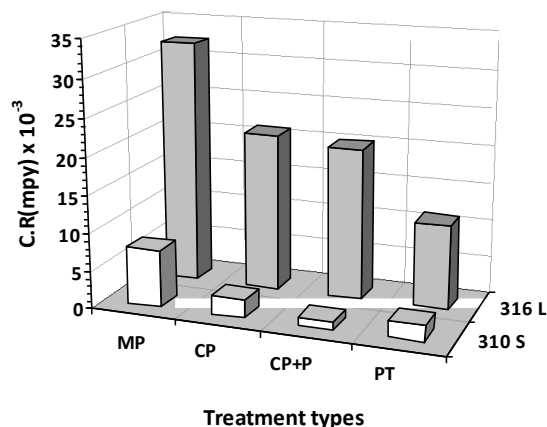


Fig. 3. Corrosion rate for AISI 316 L and AISI 310 S Stainless Steel at different treatment conditions in Hank's solution.

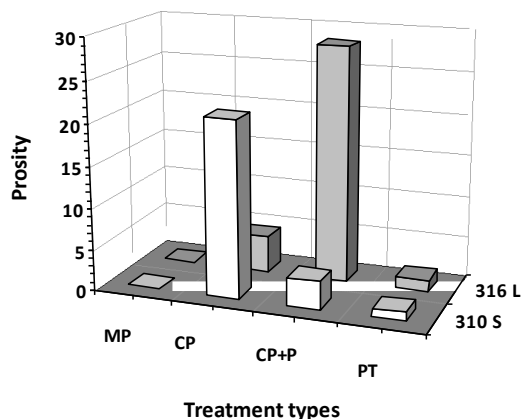
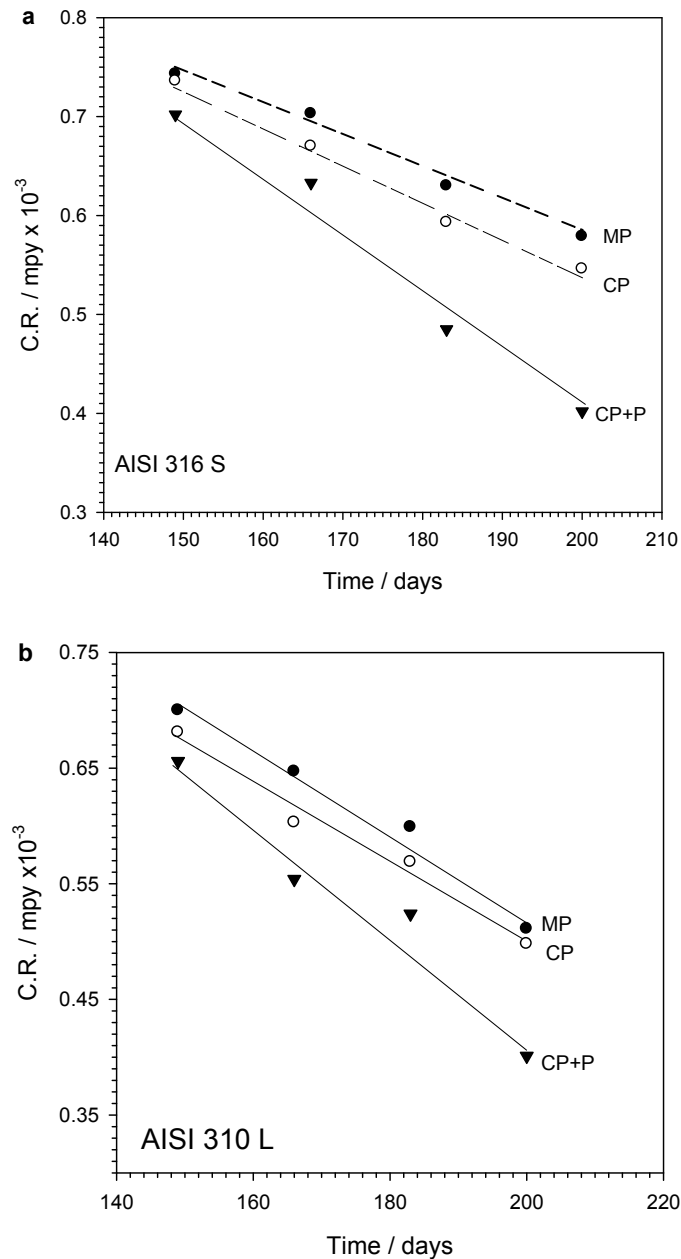


Fig. 4. Surface porosity of AISI 316 L and AISI 310 S Stainless Steel types at different treatment conditions.

Table 4. Electrochemical corrosion parameters for each treatments surface of both austenitic stainless steel in Hank's solutions as a function of pretreatment at 37°C.

316L	$E_{oc}$ V(SCE)	$E_{corr}$ V(SCE)	$E_{bd}$ V(SCE)	$R_p$ $\Omega \text{ cm}^2$	$I_{corr}$ $\mu\text{A cm}^{-2}$	$I_{bd}$ $\mu\text{A cm}^{-2}$	$\beta_a$ $\text{mV dec}^{-1}$	$\beta_c$ $\text{mV dec}^{-1}$	CR $\text{mpy } 10^{-3}$
MP	-0.464	-0.464	0.269	-0.886	1.56	51.611	236	-139	32.39
CP	-0.395	-0.403	0.378	-3.933	1.01	20.775	332	-166	20.97
CP+P	-0.298	-0.384	0.398	-25.203	0.97	1.135	610	-278	20.14
PT	-0.175	-0.178	0.408	-1.228	0.54	4.745	235	-203	11.21
310S									
MP	-0.130	-0.135	0.793	-4.835	0.365	3.590	292	-232	7.58
CP	-0.102	-0.124	1.096	-102.725	0.116	0.757	489	-305	2.39
CP+P	0.078	0.088	1.357	-16.590	0.053	0.164	375	-360	1.10
PT	0.041	0.035	1.329	-5.255	0.101	0.242	238	-214	2.10



**Fig. 5. Corrosion rate deduced from Weight loss data at different treatment conditions in Hank's solution (a) AISI 316 L SS and (b) AISI 310.**

formed presents the lowest corrosion rate (weight loss) in the field of exposure to calculate the corrosion rate from metal loss we used the following Equation [36]:

$$C.R. = \frac{W_2 - W_1}{A \times d \times t} \quad (4)$$

Where ( $W_2$ ,  $W_1$ ) is weight before and after exposure periods, ( $A$ ) is area, ( $d$ ) is density and ( $t$ ) is immersion time.

### 3.3 SURFACE ANALYSES

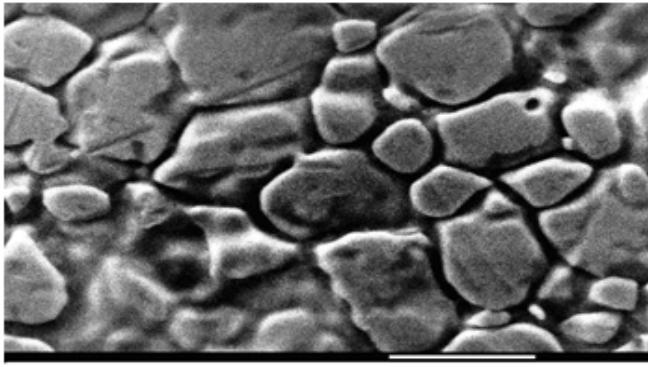
The surface morphology and XPS spectra for 316L and 310S stainless steel in hank's solution after MP, CP, CP+P and PT surfaces treatment are generally consistent with the above electrochemical behavior. The resolution XPS data are summarized in Table 5. This information was used to deduce the changes in surface chemistry that occur as a result of the surface treatments employed. XPS spectrum of SS types exhibit various peaks pertinent to the elements composing the

sample, For both the alloys, the content of the elements in decreasing order were: Fe > Cr > Ni. The total content of these as shown in Table 5.

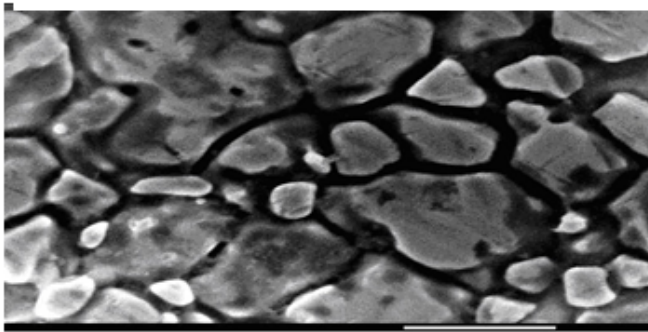
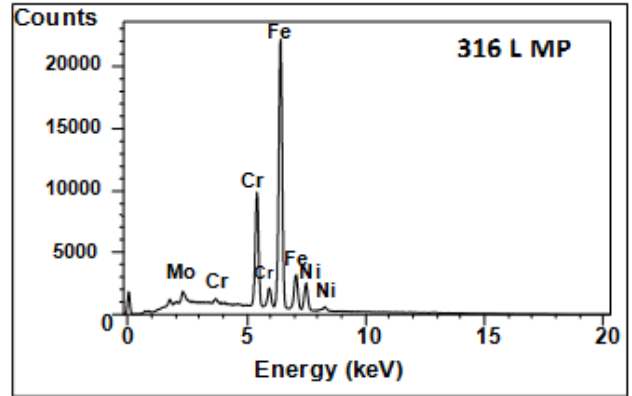
**Table 5. XPS data and Composition of surface film after each surface treatment for both austenitic stainless steel in mass percent.**

316 L	Fe Ka	Fe Kb	Cr/Fe	Cr Kesc	Cr Ka	Cr Kb	Ni Ka	Ni Kb	Mo L1	Mo La1
MP	56.4	7.3	0.273	0.8	23.7	3.5	6.3	0.7	1.3	-
CP	56.4	7.4	0.431	0.2	23.7	3.6	6.2	0.8	1.6	-
CP+P	56.9	7.5	0.432	0.2	24.1	3.5	6.3	-	0.1	1.4
PT	56.2	7.7	0.445	-	23.8	3.5	6.5	0.9	1.4	-
310 S										
MP	47.6	6	0.466	-	26.7	4.3	13.3	1.8	0.3	-
CP	45.5	6.1	0.688	-	31	4.5	11.1	1.6	0.3	-
CP+P	47.1	6	0.637	-	29.6	4.2	11.4	1.7	0.1	-
PT	44.8	6.1	0.717	-	32	4.5	10.9	1.4	0.3	-

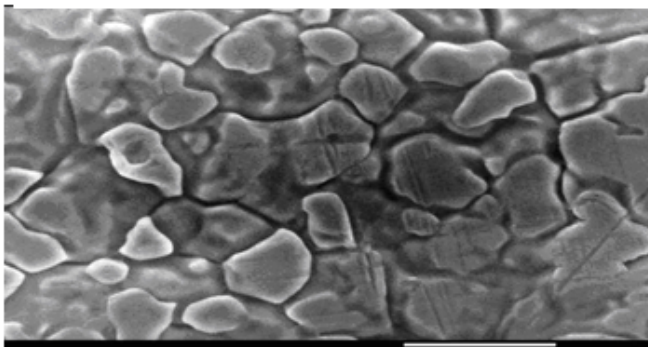
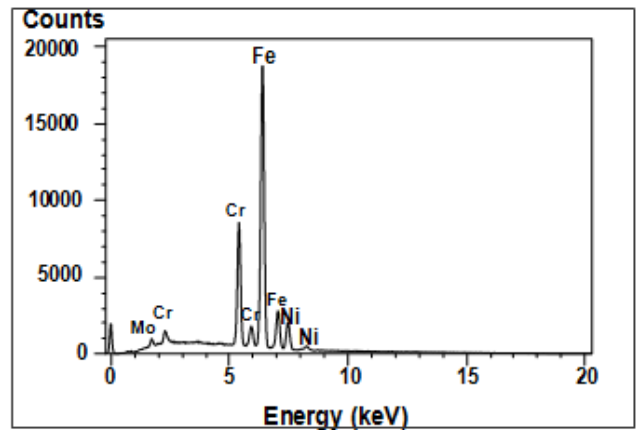
The Cr increase in surface samples after CP, CP+P and PT than the sample treated by MP in 316 L only is accomplished by increasing corrosion resistance of these samples is due to two different mechanisms according to treatment types. The first one is for samples treated by CP and CP+P, suggesting that the surface passive film is formed by a mixture of oxides [37] representing these elements. The passive film consists of water molecules, cations, anions and highly oxidized metal, such as Fe, Cr. The thickness of the passive layer ranges from a few nanometers to 10 nm. The ambient medium (wet air) reacts with metallic surfaces, especially with Cr which is more easily oxidizable than iron. Several structure models of the passive film have been proposed [38], two types being mainly mentioned,  $(Fe,Cr)_2O_3$  and  $(Fe,Cr)(OH)_n$ . When mechanically polished the sample surfaces, the characteristics of the oxygen bonds changed. There was a drop in oxygen bonding in the oxide form and a dramatic increase in oxygen bonding as a hydroxide. The chemical composition of Cr on the surface also changed with chemical polishing. In mechanically polished samples Cr was bound primarily in the oxide form ( $Cr_2O_3$ ). After chemical polishing, the proportion of Cr in the hydroxide form increased significantly through the majority of the Cr was still bound as an oxide. Chemical polishing also caused a change in the binding of the Fe on the surface. There was a decrease in metallic Fe, and an increase in Fe bound as FeO, which is adherent to the steel substrate. This was offset by a drop in Fe bound as  $Fe_2O_3$  and the hydroxide. However, more than 50% of Fe is still bound as  $Fe_2O_3$ . The Cr/Fe ratio in these samples increases after surface treatment by CP and CP+P, leading to an "enrichment" of Cr on the surface. It must be pointed out that the Cr/Fe ratio for the mechanically polished samples also indicates surface enrichment of Cr, as compared to the bulk, probably due to preferential atmospheric oxidation of the Cr. As shown in Table 5 CP+P can result in further enrichment of Cr as  $Cr_2O_3$  on the surface. Further analysis is necessary to determine the exact composition. It resulted also, in FeO concentration increasing and the Fe,  $Fe_2O_3$  and Fe-OOH concentrations decreasing. The Cr increase in SS 316L after all surface treatments and this is agreed with Hyniewicz [39]. Some researchers [40] suggested that the improved corrosion behavior of 316L can be attributed to an increase in Cr and other elements contributing to the formation of the passive film. Based on the surface analysis, a three-layer model has been suggested for passive films formed on austenitic stainless steel in acid solutions: the outer part of the film consists of a hydroxide film on top of an oxide layer [41]. The oxy-hydroxide film is formed on top of a Ni-enriched layer, the origin of which is the selective oxidation of Fe and Cr during anodic polarization [40].



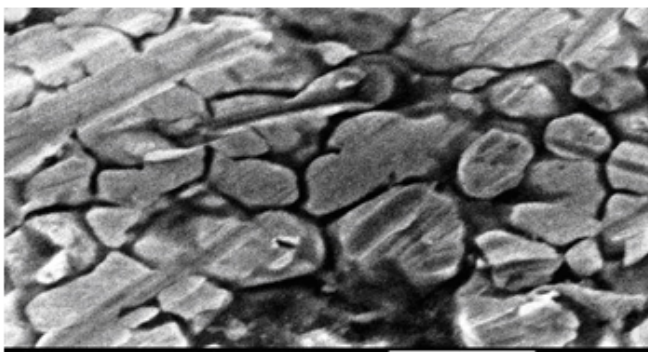
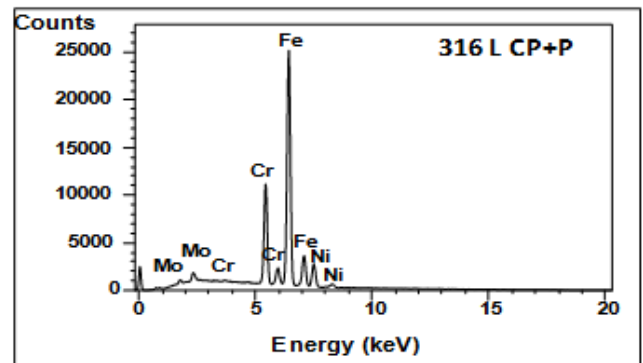
316 L MP X5.000 5 μm



316 L CP X5.000 5 μm



316 L CP+P X5.000 5 μm



316 L PT X5.000 5 μm

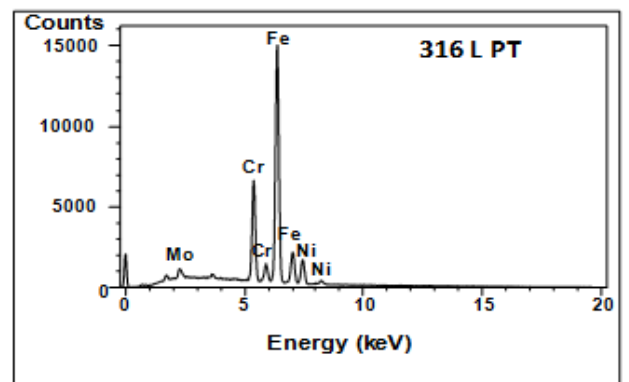


Fig. 6. SEM micrographs and EDX surface analysis of AISI 316 L stainless steel at different treatment conditions after polarization in Hank's solution.

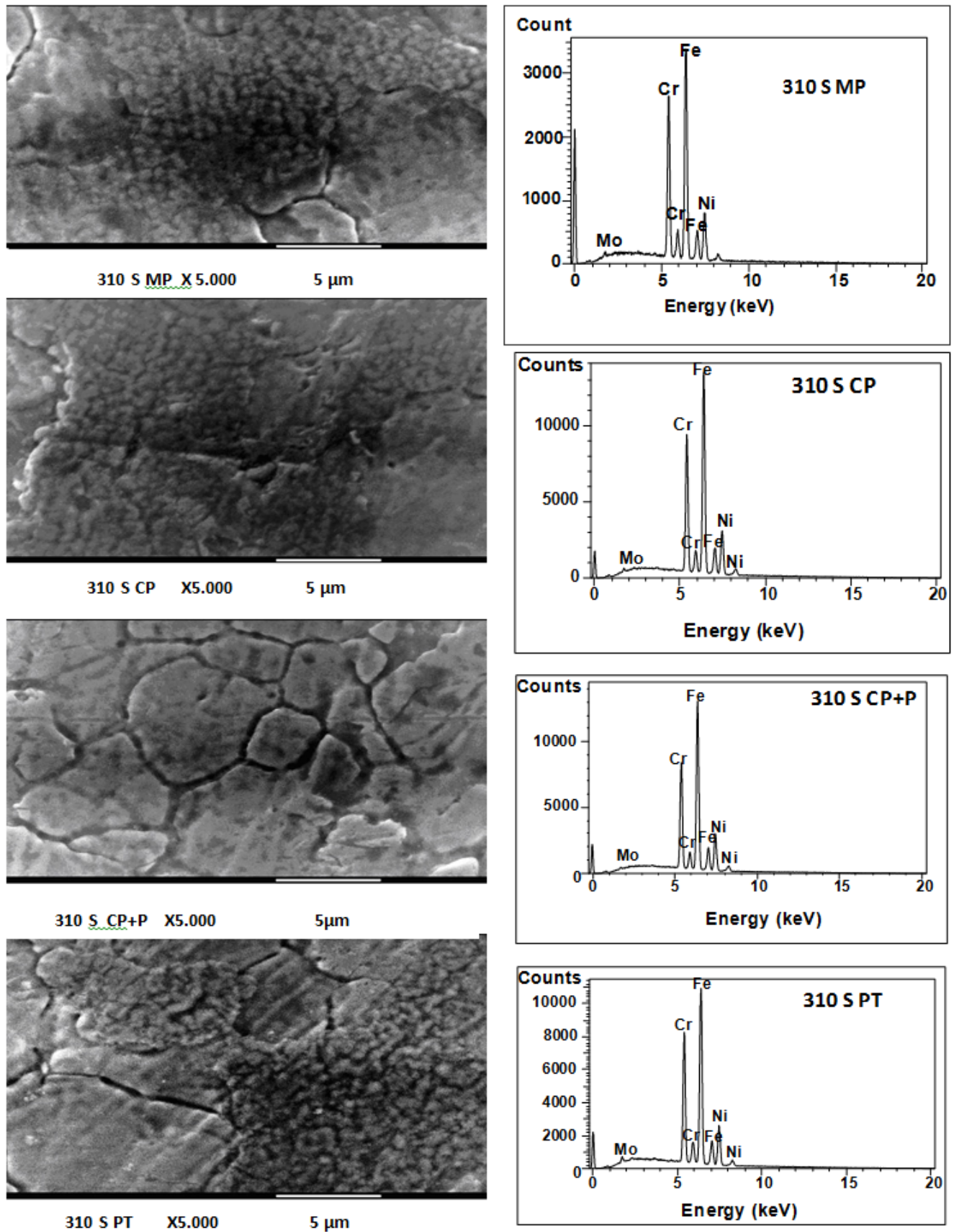


Fig. 7. SEM micrographs and EDX surface analysis of AISI 310 S stainless steel at different treatment conditions after polarization in Hank's solution

Total Ni % which surface contains changed from 7% after MP, and CP, 6.3% after CP+P and 7.4% after PT in AISI 316 L, while in 310 S 1 5.1 after MP, 12.7% after CP, 13.1% after CP+P and 12.3% after PT. Benard [42] has shown that, the Ni was not present in the products formed at the start oxidation of austenitic steels; since Ni is more noble than Fe, it would be rejected to the metal/oxide interface. This phenomenon is confirmed by the concentration of Ni in the Cr depleted region. For biomedical applications this can be a desirable finding as nickel has been known to cause allergic reactions in some individuals. Other [41] have proposed that immersion in nitric acid removes sulfide inclusions of the stainless steel thus eliminating preferential sites for corrosion attack. The practical use of the nitric acid treatment might be limited if the treatment leads to formation of a Cr-depleted zone underneath the passive film, since damage of the passive film leads to Cr-depleted zone exposure to the environment. The atomic ratio Cr/ (Cr+Fe+Ni) under the passive film was found to vary between 20-25% in the passivation treated samples which somewhat higher than in the bulk (20%). On other hand, Ni-enrichment was detected and Fe was found to be depleted. The results suggest that Fe is selectively dissolved during the passivation treatment and Cr does not seem to be depleted underneath the passive film [43]. The XPS results represent that increase Cr percentage in the surface of both stainless steel types after plasma treated PT is good qualitative agreement with the enhance the corrosion resistance after plasma from polarization and weight loss results, is due to second mechanism occurred.

It is known that if the stainless steel samples are treated by plasma under 400°C-450°C, nitrogen rich iron phase ( $\gamma^N$ ) that is called S-phase will be formed [44]. This phase is characterized by its corrosion resistance due to the compressive stress that is formed inside it. If the treatment temperature increases above 500°C, the CrN phase starts to grow along the grain boundaries of the stainless steel. The CrN phase is increase the corrosion resistance, is due to the fact that nitrogen atom in the nitride layer firstly dissolved into the solution, and it could repel the chloride ion (Cl<sup>-</sup>) away from the sample surface. The nitrogen anion (N<sup>-</sup>) then combines with hydrogen ion (H<sup>+</sup>) in the solution to form the ammonium (NH<sub>4</sub><sup>+</sup>) resulting increase of solution pH. Finally, corrosion attack from the solutions decreases [45-47].

Fig. 6 shown that the grain size of SS 316L is affected by type of surface treatments, as can be seen the grain size of untreated by chemical polishing CP or passivity CP+P or plasma treated PT are greater than treated surface, the small grain size appear after CP+P. It can be also seen the distortion of the grains of the stainless steels after PT and the surface of all SS 316 L samples have a crystalline structure after all treatment types. While in Fig. 7 the grain size of SS 310S is affected by type of surface treatments, as can be seen the grain boundary of MP and CP samples are not clear as in sample treated by CP+P and PT, the big grain size appear after CP+P. It can be also seen the grain size decreases after plasma treatment and treatment types change the amorphous to crystalline structure of the surface of SS 310 S. The morphology of SS 316 L and 310 S austenitic SS is different although it has the same main component at different ratio. From SEM photographs of both stainless steel samples treated by plasma, it can be noticed a distortion of the grains of the stainless steels as shown in 316 L samples. The grain size decreases as in the case of 310 S samples. this behavior is due to the bombardment of the nitrogen and hydrogen positive ions, that are formed in the plasma discharge, on the sample surface which causes the crystalline of the stainless steels will change to be nano-crystals or even amorphous. In some cases this change of the grain size improves the corrosion resistance of the stainless steels [17].

#### 4 CONCLUSION

It can be concluded that different types of treatments affected the electrochemical behavior of samples. Every stainless steel sample has lower corrosion current density  $I_{corr}$  has lower corrosion rate that occurred maximum breakdown potential  $E_{bd}$  for both SS types sample and this mean improve corrosion resistance of this samples. These results are in good agreement with corrosion rate calculated by weight loss test. OCP of AISI 316 L display that, the PT is shifted to noble direction than CP+P, CP, MP respectively. While the value of OCP of AISI 310S display that the CP+P is shifted to noble direction than PT, CP, MP respectively. The passivation treatment significantly increases the corrosion resistance due to a high Cr content in the passive film and increased film thickness. From the results it can be concluded the AISI 310 S have higher corrosion resistance than AISI 316 L, so it can be recommend use it in biomedical application as 316 L which widely used biomaterials .

#### REFERENCES

- [1] I. Gurappa, Characterization of different materials for corrosion resistance under simulated body fluid conditions, J. Materials Characterization 49 (2002) 73–79.
- [2] C.V. Vidal, A.I. Muñoz, Electrochemical characterisation of biomedical alloys for surgical implants in simulated body fluids, Corrosion Science 50 (2008) 1954–1961.

- [3] M. Sumita, T. Hanawa and D. H. Teoh: Development of nitrogen-containing nickel-free austenitic stainless steels for metallic biomaterials-review, *Mater. Sci. Eng., C24* (2004) 753-760.
- [4] B.D. Ratner, A.S. Hoffman, F.J. Schoen, J.E. Lemons, *Biomaterials science: an introduction to materials in medicine*. San Diego: Elsevier/Academic Press (2004).
- [5] A.C. Fraker, *Corrosion of metallic implants and prosthesis devices*. In: *ASTM metals handbook* (9th ed.) Corrosion. Metals Park, OH: ASM International, 13 (1987) 1324–35.
- [6] M.F. Leclerc, *Surgical implants*. In: *ASTM metals handbook* (9th ed.) Metals Park, OH: ASM International 2 (1987) 164–80.
- [7] J.J. Jacobs, J.L. Gilbert, R.M. Urban, *Current Concepts Review - Corrosion of Metal Orthopedic Implants*, *J. Bone Joint Surg* 80-A (1998) 268–82.
- [8] S.G. Steinemann, *Metal implants and surface reactions*, *Injury* 27:SC (1996) ,16–22.
- [9] M. Donachie, *Biomedical alloys.*, *Adv Mater Process* 7 (1998) 63– 65.
- [10] H. Yang, K. Yang, B. Zhang, *Pitting corrosion resistance of La added 316L stainless steel in simulated body fluids*, *Mater. Lett.* 61 (2007) 1154–1157.
- [11] Y. Nakayama, T. Yamamura, Y. Kotoura, M. Oka, *Measurement of anodic polarization of orthopaedic implant alloys: comparative study in vivo and in vitro experiments* *J. Biomaterials* 10 (1989) 420.
- [12] M. Morita, N. Nakamura, Y. Tsukamoto, T. Sasada, *J. Jpn. Soc. Biomater*, 10 (1992) 209-212.
- [13] H. Bidhendi and M. Pournavari, *Corrosion study of metallic biomaterials in simulated body fluid*, *Metalurgija-M J o M* 17 (2011) 13-22.
- [14] M. talha, C.K. Behera and O.P. Sinha, *Potentiodynamic polarization study of Type 316L and 316LVM stainless steels for surgical implants in simulated body fluids*, *Journal of Chemical and Pharmaceutical Research*, 4 ( 2012) 203-208.
- [15] M. Sumita, *Orthop. Surg.*, 48 (1997) 927.
- [16] Y. Okazaki, E. Gotoh, *Metal Release from Stainless Steel, Co-Cr-Mo-Ni-Fe and Ni-Ti Alloys in Vascular Implants* *Corros. Sci.*, 50 (2008) 3429–3438.
- [17] S. Mukherjee, et al, *Effect of Plasma Nitriding and Nitrocarburising Process on the Corrosion Resistance of Grade 2205 Duplex Stainless Steel*,13th International Conference on Plasma Surface Engineering Garmisch- Partenkirchen, Germany, September 10-14 (2012).
- [18] A. Shahryari, S. Omanovic, J. A. Szpunar, *Electrochemical formation of highly pitting resistant passive films on a biomedical grade 316LVM stainless steel surface* *Materials Science and Engineering C* 28 (2008) 94–106.
- [19] C. Tang, S. Katsuma, S. Fujimoto, S. Hiromoto, and *316L stainless steels in simulated body fluids and cell cultures*, *Acta Biomaterialia*, 2 (2006) 709–715.
- [20] C.C. Shih, C.M. Shih, Y.Y. Su, L.H.J. Su, M.S. Chang and S.J. Lin, *An impedance study of two types of stainless steel in Ringer physiological solution containing complexing agents*, *Corrosion. Sci.*, 46 (2004) 427.
- [21] H.D. Pletka, U. Reichau and K.G. Schutze, *Surface treatments to improve corrosion resistance of austenitic stainless steels*, *Prog.Un-der & Pre.Corros.*, bf2 (1993) 1101.
- [22] J.F. Grubb, J. Fritz and R.E. Polinski *US Patent, No.6709528* (2004).
- [23] H.A. Videla, *Microbially induced corrosion: An updated overview*. In: *Biodeterioration and Biodegradation*, H.W. Rossmore (ed.). London: Elsevier Applied Science, London, pp 63-88ce. (1991).
- [24] Little, B.J., Wagner, P. Hart, K., Ray, R., Lavoie, D., Neelson, K. & Aguilar, C. *The role of metal-reducing bacteria in microbiologically influenced corrosion*. Paper No. 215, *Proc. Nace Corrosion*. Houston, TX: National Association of Corrosion Engineers International (1997).
- [25] F. El-Taib Heikal, A.M. Fekry, A.A. Ghoneim, *Corrosion characterization of new tin–silver binary alloys in nitric acid solutions*, *Corros. Sci.*, 50 (2008) 1618-1626.
- [26] L.L. Shreir, ed., *Corrosion Metal/Environment Reactions*, Vol. I, New-Butterworth, Boston (1976).
- [27] S. Luiz de Assis, S. Wolynec, I. Costa, *Corrosion characterization of titanium alloys by electrochemical techniques*, *Electrochim. Acta*, 51 (2006) 1815-1819.
- [28] W.Y. Guo, J. Sun, J.S. Wu, *Electrochemical and XPS studies of corrosion behavior of Ti–23Nb–0.7Ta–2Zr–O alloy in Ringer's solution*, *Mater. Chem. Phys.*, 113 (2009) 816-820.
- [29] K.Salma, L. Berzina-Cimdina, N. Borodajenko, *Influence of calcium phosphate synthesis parameters on properties of bioceramics*, *Processing and Application of Ceramics*, 4(2010) 45.
- [30] G.T. Burstein, *Size and Solid Solubility in Electrodeposited Ag-Ni Nanoparticles*, *Corros. Sci.* 47 (2005) 2858–2870.
- [31] G. Wu, Y. Fan, A. Atrens, C. Zhai, W. Ding, *Electrochemical behavior of magnesium alloys AZ91D, AZCe2, and AZLa1 in chloride and sulfate solutions*, *J. Appl. Electrochem.* 38 (2008) 251–257.
- [32] J. Liang, P. Bala Srinivasan, C. Blawert, W. Dietzel, *Influence of chloride ion concentration on the electrochemical corrosion behaviour of plasma electrolytic oxidation coated AM50 magnesium alloy*, *Electrochim. Acta* 55 (2010) 6802–6811.

- [33] J.Reeve, G Nielsen, The Stern-Geary method. Basic difficulties and limitations and a simple extension providing improved reliability, 13,5(1973) 351.
- [34] W.Tato, D.Landolt, Electrochemical Determination of the Porosity of Single and Duplex PVD Coatings of Titanium and Titanium Nitride on Brass J. Electrochem. Soc. 145 (1998) 4173.
- [35] J.C. Caicedo, C. Amaya, G.Cabrera, J.Esteve, W. Aperador, M. E. Gomez, P. Prieto. Corrosion surface protection by using titanium carbon nitride/titanium–niobium carbon nitride multilayered system, Thin Solid Films Thin Solid Films 519 (2011) 6362.
- [36] Jan. 1, ASTM D2688 Standard Test Method for Corrosively of Water in the Absence of Heat Transfer (Weight Loss Method) Current edition approved Published January 2005.
- [37] J. Kruger, Passivity in ASM Handbook Volume 13A Corrosion: Fundamentals, Testing and Protection, S.Cramer & B.Covino Editors, ASM International, 2003, p61-67. M.F. López, A. Gultiérrez, J. A. Jiménez, Surf. Sci., 482-485 (2001) 300-305.
- [38] M. Pourbaix Atlas d'équilibres électrochimiques, Gauthier-Villars, Paris, 1963; English translation: Atlas of electrochemical, Equilibria in aqueous Solutions, Pergamon Press, Oxford, 1966.
- [39] T. Hryniewicz, R. Rokicki, K. Rokosz, Corrosion Characteristics of Medical-Grade AISI Type 316L Stainless Steel Surface After Electropolishing in Magnetic Field, Corrosion, (The Journal of Science and Engineering), Corrosion Science Section Corrosion Science Section 8 (2008) 660-665.
- [40] O. A. Olsson, D. Landolt, Passive films on stainless steels-chemistry, structure and growth, Electrochimica Acta 48 (2003) 1093-1104.
- [41] P. Stefanov, D. Stoychev, M. Stoycheva, T. Marinova, Chromium Oxide Films Chemically Formed on Stainless Steel 316L, Mat. Chem. Phys Mat. Chem. Phys. 65 (2000) 212-215
- [42] J. BENARD Oxydation des métaux [Oxidation of metals] Pub. Gauthier Villars Paris, 1962 J. Benard, Oxydation des métaux [Oxidation of metals] Pub. Gauthier Villars Paris, 1962
- [43] D. Wallinder, J. Pan, C. Leygraf, A. Delblanc-Bauer, EIS and XPS study of surface modification of 316LVM stainless steel after passivation Corrosion Sci. 41 (1998) 275-289.
- [44] Z. Yu, L. Wang, X. Xu and J. Qiang, Growth Process of Low-Temperature Plasma-Nitriding Layer on Austenitic Stainless Steel, Acta Metallurgica Sinica (English letters) 17, 2 (2004) 210-214
- [45] S. D. Chyou, H.C. Shih, The Effect of Nitrogen on the Corrosion of Plasma-Nitrided 4140 Steel, Corrosion, 47,1 (1991) 31-34.
- [46] A. Triwiyantol, P. Hussain, M. C. Ismail, Behavior of Carbon and Nitrogen after Low Temperature Thermochemical Treatment on Austenitic and Duplex Stainless Steel, Applied Mechanics and Materials 110 (2012) 621-626.
- [47] H. J. Grabke, High Nitrogen Steels. The Role of Nitrogen in the Corrosion of Iron and Steels, ISIJ. International, 36, 7(1996) 777-786.